

3D Time Dependent Stokes Vector Radiative Transfer in an Atmosphere-Ocean System Including a Stochastic Interface

George W. Kattawar
Dept. of Physics
Texas A&M University
College Station, TX 77843-4242
phone: (979) 845-1180 fax: (979) 845-2590 email: kattawar@tamu.edu

Award #: N000141110154
<http://people.physics.tamu.edu/trouble/work.html>

LONG-TERM GOALS

The major objective of this proposal is to calculate the 3-D, time dependent radiation field both within the ocean and in the atmosphere in the presence of a stochastically varying interface which may also be perturbed by sea foam, air bubbles, surfactants, rain, etc. This study will serve as the genesis to the future evolution of an inversion algorithm whereby one could reconstruct images that have been distorted by the interface between the atmosphere and the ocean or the ocean itself. This study will rely heavily on both the spectral and polarimetric properties of the radiation field to deduce both the sea state and the perturbations produced on it. A second phase of this study will be to explore the asymptotic polarized light field and to determine how much information can be obtained about the IOP's of the medium by measuring it. The third phase of this proposal will deal with the problem of improving image resolution in the ocean using some novel polarimetric techniques that we are just beginning to explore. Once these studies have been completed using a passive source, it will be rather straightforward to extend them to active sources where we can explore the use of both photo-acoustic and ultrasound-modulated optical tomography to improve image resolution.

OBJECTIVES

The new Navy initiative is focusing on one of the most formidable problems in radiative transfer theory; namely, calculating the full 3D time dependent radiation field (with full Mueller matrix treatment) in a coupled atmosphere-ocean system where the boundary separating the two has both spatial and temporal dependence. Although a great deal of work has been done on obtaining power spectra for ocean waves, I know of no work that has yielded similar results for the radiation field within the ocean. It is clear that as long as the surface has a significant effect on the internal light field, it will leave its signature on the radiation field within the ocean and the relative strength of this field compared to the ambient field will determine the success or failure of inversion algorithms. However, as we go deeper within the ocean we start to enter a region called the asymptotic region where all photons lose memory of their origin and the light field then remains stationary and becomes independent of the azimuthal angle. The depth dependence becomes simply exponential, i.e. $L(z+h, \theta) = L(z, \theta) \exp(-kh)$ where k is called the diffusion exponent. It should be noted at this juncture that this asymptotic light field is still polarized which is why we used the bold-faced vector notation. We were the first to compute the degree of polarization for this asymptotic light field for Rayleigh scattering and

Report Documentation Page				Form Approved OMB No. 0704-0188	
Public reporting burden for the collection of information is estimated to average 1 hour per response, including the time for reviewing instructions, searching existing data sources, gathering and maintaining the data needed, and completing and reviewing the collection of information. Send comments regarding this burden estimate or any other aspect of this collection of information, including suggestions for reducing this burden, to Washington Headquarters Services, Directorate for Information Operations and Reports, 1215 Jefferson Davis Highway, Suite 1204, Arlington VA 22202-4302. Respondents should be aware that notwithstanding any other provision of law, no person shall be subject to a penalty for failing to comply with a collection of information if it does not display a currently valid OMB control number.					
1. REPORT DATE 2012		2. REPORT TYPE N/A		3. DATES COVERED -	
4. TITLE AND SUBTITLE 3D Time Dependent Stokes Vector Radiative Transfer in an Atmosphere-Ocean System Including a Stochastic Interface				5a. CONTRACT NUMBER	
				5b. GRANT NUMBER	
				5c. PROGRAM ELEMENT NUMBER	
6. AUTHOR(S)				5d. PROJECT NUMBER	
				5e. TASK NUMBER	
				5f. WORK UNIT NUMBER	
7. PERFORMING ORGANIZATION NAME(S) AND ADDRESS(ES) Dept. of Physics Texas A&M University College Station, TX 77843-4242				8. PERFORMING ORGANIZATION REPORT NUMBER	
9. SPONSORING/MONITORING AGENCY NAME(S) AND ADDRESS(ES)				10. SPONSOR/MONITOR'S ACRONYM(S)	
				11. SPONSOR/MONITOR'S REPORT NUMBER(S)	
12. DISTRIBUTION/AVAILABILITY STATEMENT Approved for public release, distribution unlimited					
13. SUPPLEMENTARY NOTES The original document contains color images.					
14. ABSTRACT					
15. SUBJECT TERMS					
16. SECURITY CLASSIFICATION OF:			17. LIMITATION OF ABSTRACT SAR	18. NUMBER OF PAGES 12	19a. NAME OF RESPONSIBLE PERSON
a. REPORT unclassified	b. ABSTRACT unclassified	c. THIS PAGE unclassified			

were able to obtain an analytic expression for both the polarized radiation field and the diffusion exponent (see ref. 1). In addition, we were also able to set up a numerical scheme to compute the polarized radiation field as well as the diffusion exponent for any single scattering Mueller matrix. The interesting feature about the asymptotic light field is that it depends profoundly on both the single scattering albedo as well as the phase function of the medium. We also found that substantial errors will occur in both the ordinary radiance and the diffusion exponent if they are calculated from scalar rather than vector theory

APPROACH

There are several stages to our approach that we will enumerate. The sine qua non for this entire project will be the development of a fully time dependent 3-D code capable of calculating the complete radiation field, i.e. the complete Mueller or Green matrix at any point within the atmosphere-ocean system. This of course implies that both horizontal as well as vertical IOP's must be accounted for. It should also be noted that the code must be capable of handling internal sources as well in order to explore both fluorescence and bioluminescence. At present there are several 3D codes that are able to compute various radiometric quantities in inhomogeneous media; however, as far as we know, none exists which will couple both atmosphere and ocean with a time dependent stochastic interface. One of the earliest 3D radiative transfer (RT) codes was developed by Stenholm, et. al.² to model thermal emission from spherical and non-spherical dust clouds. It was based on an implicit discretization of the transfer equation in Cartesian frames. To our knowledge, the first 3D-scalar RT code using discrete ordinates was written by Sánchez³ et al.; however, it did not make use of spherical harmonics and lacked efficiency and accuracy particularly for small viewing angles. The addition of polarization to the 3D discrete ordinates method was done by Haferman⁴ et al. Almost concurrently, a 3D-scalar RT code was written by K. F. Evans⁵ which used both spherical harmonics and discrete ordinates. This method uses a spherical harmonic angular representation to reduce memory and CPU time in computing the source function and then the RT equation is integrated along discrete ordinates through a spatial grid to model the radiation streams. We have already obtained this code and will use it for validation of our 3D scalar Monte Carlo code for both the atmosphere and ocean components. Several Monte Carlo codes both scalar and vector have been published for solving specialized problems in atmospheric optics usually dealing with finite clouds^{6,7,8,9}. Without exception, these codes are using quite primitive, also called "brute force", methods. None of them will do what we are proposing in our approach to the fully time dependent 3D solution applicable to both atmosphere and ocean. It should be mentioned that we have already successfully added to our Green matrix Monte Carlo code the capability to handle internal sources such as fluorescence, bioluminescence and even thermal emission.

Once we have developed our 3D code to handle both the ocean and atmosphere without the interface included, we will then develop a 3D form of 1D matrix operator theory that we worked out in two seminal papers published in *Applied Optics*^{10,11}. The basic idea of the method is that if one knows the reflection and transmission operators of say two layers, then it is rather straightforward to get the reflection and transmission operators for the combined layer. With this method we can start from an infinitesimal layer and build large and even semi-infinite layers in a rapid way, i.e. if we start with a layer of thickness Δ then in N steps we can reach a thickness of $2^N \Delta$. Another very relevant feature of this method is that it will allow us to add the interface to the "bare" ocean, i.e., one without an interface, to get the combined ocean-interface operator and then add this layer to the atmosphere for the final reflection and transmission operators for the combined system. The question immediately

arises is why not solve the entire system at the same time? The answer is that by doing it this way we only have to use the adding feature to combine the time dependent interface thus avoiding performing the entire calculation at each instant in time. This method has also become known as the adding-doubling method. These operators are effectively the impulse response or Green matrix for the upper and lower boundaries of the medium. Therefore, if we know the external radiance input into both upper and lower layers, we can then obtain the output at both the upper and lower boundaries of the combined system. A pictorial description of the method is shown in Fig. 1. It should be emphasized that this method will also handle internal sources as well such as bioluminescence, fluorescence, and even thermal emission. This method can also handle detectors at any interior point in the medium. Another bonus of matrix operator theory is that one can easily obtain the path radiance between source and detector which is a sine qua non for image analysis.

In order to add a interface which is spatially inhomogeneous in the y direction but homogeneous in the x direction, we will need the reflection (R) and transmission (T) operators for both the atmosphere and ocean now as a function of time t and both z and y ; namely $R(y-y_0, z, t, \theta, \phi)$ and similarly for T . It is important to note that we only have to obtain the response of the atmosphere or ocean to a single line source at the point y_0 and then using the translational invariance of the medium in the y -direction will have the reflection and transmission operators at every point in the y -direction. The only method we know to create these 2-D operators is Monte Carlo. Once these are obtained, we can use the output from each layer as the input to the surface boundary whose reflection and transmission properties are either known or calculable. For instance if the surface consists of just capillary or gravity waves, then we just need the Fresnel coefficients to give us the requisite reflection and transmission operators for the interface. Now once these operators are obtained then we can use extended matrix operator theory to get the final time dependent radiation field that a detector will see. Let us consider the simplest case where the surface is 1-D and we know its power spectrum. It should be emphasized at this point that it is not sufficient to have just a wave-slope distribution since it will only give us statistically averaged results for the radiance field. The introduction of the spatial and temporal dependent interface destroys the symmetry and makes all 1-D codes essentially useless in this domain. At each instant in time, the surface will have a distinct shape that will evolve in time. We have developed a method using linear filter theory whereby we can take an ocean power spectrum and using a random number generator create a realistic surface that will match the original power spectrum and will still exhibit both stationarity and ergodicity. Now the nice feature about what we are proposing is that we can now concentrate on just the effects of the surface on the detectors since as the surface evolves in time so too will the radiance field as recorded by the detectors. Now both the spatial and temporal profiles will be constantly changing; however, we will have created them from a medium which has been assumed stationary and only the interface produces the time dependence and the horizontal spatial inhomogeneities, i.e. the R and T operators for both the atmosphere and ocean need only to be computed **once**. This is clearly a first-order solution to the more complex problem; however, it should tell us a great deal about future complexities of inversion and also the efficacy of pursuing the next level of difficulty. If the surface is perturbed by foam, bubbles, etc. then these can be added and the matrix operator theory will be used to calculate the effective reflection and transmission operators of the perturbed surface. It should also be stated that this project is enormously computationally intensive; however, the type of codes we will produce are ideally suited for large-scale parallel processors, which we do have access to.

The next level of difficulty is where we will use Monte Carlo methods to compute a full 3-D distribution of the time dependent radiation field, which now may include 3-D inhomogeneities in both

the ocean and atmosphere. This will be a computational tour de force requiring a major new computer program that must be capable of placing IOP's of both the atmosphere and ocean at each point in a large 3-D grid. Matrix operator theory will again be used but it will now be much more complicated since our reflection and transmission operators now become functions of three spatial variables. In fact, the complete solution to this problem could approach the complexity of the general circulation models used in weather forecasting. Due to the large volume of data that will be generated, we will clearly have to develop methods to easily display animated sequences of this time dependence.

These projects were worked on by Dr. Pengwang Zhai, who left for NASA Langley Research Center in August 2008, then by Dr. Yu You, who left for Schlumberger, and are now being worked on by Dong Sun, a postdoctoral research associate.

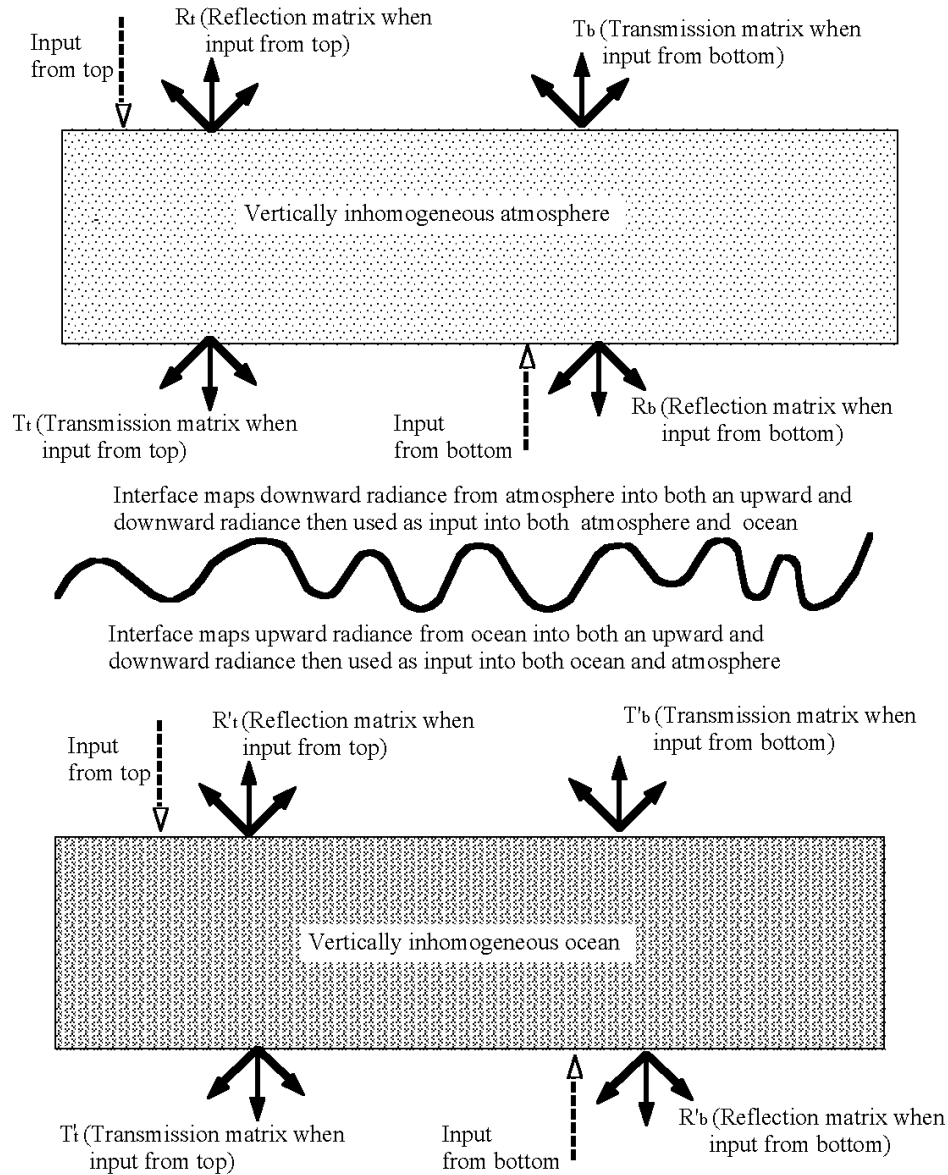


Fig. 1. Schematic representation on the use of matrix operator theory to calculate the time dependent radiation field within the ocean

WORK COMPLETED

- a) We have investigated the polarized Raman scattering in seawater with hydrosols. The code we used for this part is a modification of our previous 3D-scalar RT code and we only considered the 1D case where detectors could be placed at any location in the ocean. Due to the wavelength dependency of the absorption/scattering coefficients, we found that the Raman scattering distribution has a very strong dependency on optical depth.
- b) We are also able to calculate the “effective” Mueller matrix for Raman multiple scattering for any polarized incident light field. We investigated the effect of polarization from Raman scattering and found it can be a useful tool for remote sensing of the ocean and in particular for remote temperature determination.
- c) We have completed a lengthy review article titled “Genesis and Evolution of Polarization of Light in the Ocean” which has been accepted for publication in Applied Optics.

RESULTS

a) Raman Scattering.

The distinguished property of Raman scattering is a frequency shift between the incident light and scattered light. Water molecules will be excited by the incident light from the lowest vibrational level to virtual energy levels, and then they will decay to the first excited vibrational level with emission of longer wavelength light. The frequency of the scattered light is determined by both the incident light frequency and the energy difference between the vibrational levels. Fig.2 demonstrates the mechanism of Raman scattering in water. As a result of this property and its unique polarization properties, Raman scattering may become a very promising tool for remote sensing the oceans.

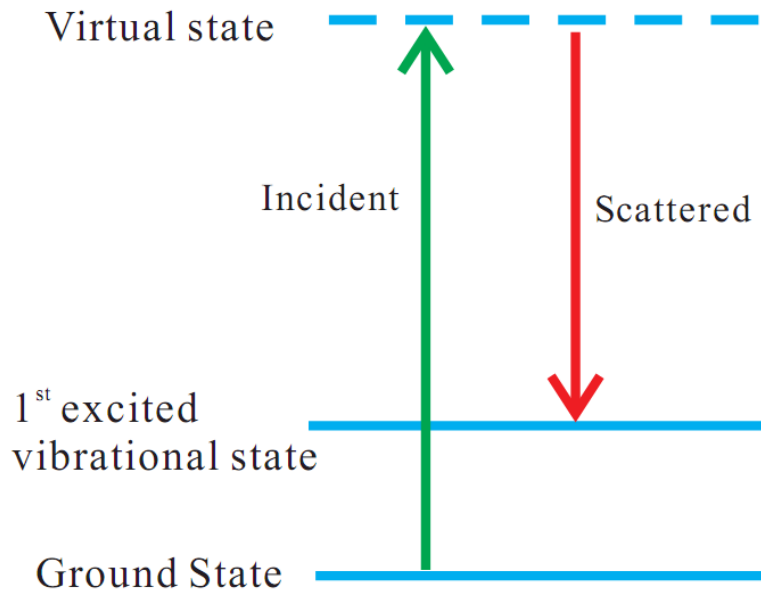


Fig.2 Raman Scattering model for water

Water molecules have very complex vibrational modes, which result in the superposition of different Gaussian distributions which lead to a complex band shape. Walrafen¹² first provided a mathematical equation to fit the experimental data of the Raman scattering band for liquid water, which is a superposition of four Gaussian functions:

$$I^R(\tilde{\nu}) = \sum_{i=1}^4 \frac{A_i}{\tilde{\nu}_i^{\sim Hw}} \exp \left(-\frac{\left(\tilde{\nu} - \tilde{\nu}_i \right)^2}{\left(\tilde{\nu}_i^{\sim Hw} \right)^2} k \right) \quad (1)$$

in which A_i is the amplitude, $\tilde{\nu}_i$ is the wavenumber of the center of each Gaussian function, $\tilde{\nu}$ is the shift of wavenumber relative to the incident light, and $\tilde{\nu}_i^{\sim Hw}$ is the FWHM for each Gaussian component, and the constant $k = 4 \ln 2$.

The values of parameters of A_i , $\tilde{\nu}_i$ and $\tilde{\nu}_i^{\sim Hw}$ at a temperature of 25°C are given in Table.1, and the band shape is given in Fig.3. It is clear to see that there is a shoulder at the shorter wavelength side of the band distribution.

Table.1

i	A_i	$\tilde{\nu}_i$	$\tilde{\nu}_i^{\sim Hw}$
1	0.65	3247	233
2	0.62	3435	176
3	0.15	3535	144
4	0.145	3622	141

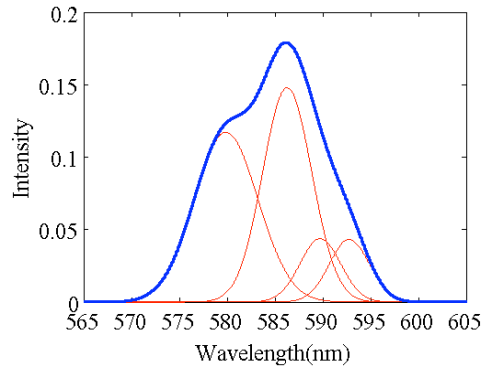


Fig.3 Raman band structure of water

To deal with polarized scattering, the Mueller matrix for single scattering is most essential. In general, it is given by Xu¹³

$$M_{rad} = \begin{pmatrix} 1 & \frac{(1-\rho)(c^2-1)}{(1+c^2)+(3-c^2)\rho} & 0 & 0 \\ \frac{(1-\rho)(c^2-1)}{(1+c^2)+(3-c^2)\rho} & \frac{(1-\rho)(c^2+1)}{(1+c^2)+(3-c^2)\rho} & 0 & 0 \\ 0 & 0 & \frac{(2-2\rho)c}{(1+c^2)+(3-c^2)\rho} & 0 \\ 0 & 0 & 0 & \frac{(2-6\rho)c}{(1+c^2)+(3-c^2)\rho} \end{pmatrix} \quad (2)$$

where $c = \cos(\theta)$ and θ is the scattering angle between incident and scattered light.
 ρ is the depolarization ratio. In the ocean, $\rho = 0.17$ for Raman scattering.

We have investigated the situation where there is particle (hydrosol) scattering in the seawater. The phase functions of Raman scattering and fluctuation scattering of seawater are already well known. The total phase function is a superposition of phase functions for pure seawater and the particle phase function.

Our algorithm is demonstrated in Fig. 4. We send in light with a wavelength of 488nm at a zenith angle of 180° . We force the first scattering to be Raman scattering with a single scattering albedo of unity. Light will be scattered to different wavelengths from 565nm to 595nm. The weight distribution of each wavelength follows Eq. (1) or Fig. 3. After that point, each scattering will be a Rayleigh scattering until the photon weight becomes less than cut-off weight. Our simulations are based on the Monte Carlo method, which uses probability density functions for each of the scattering/absorption processes occurring in the ocean. If a photon passes the sensor from top to bottom, it is called transmission, with scattering angle from 90° - 180° ; if a photon passes the sensor from bottom to top, it is called scattering, with scattering angle from 0° - 90° .

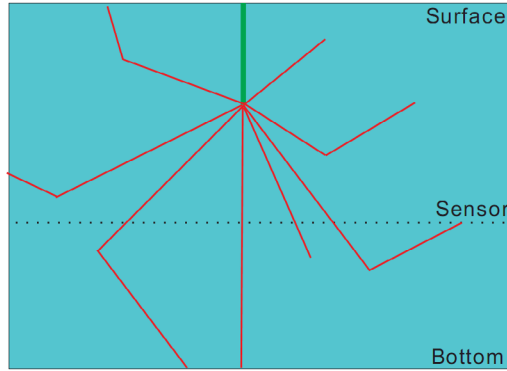


Fig.4 Raman Scattering model in seawater.
Green line is incident light with wavelength 488nm.

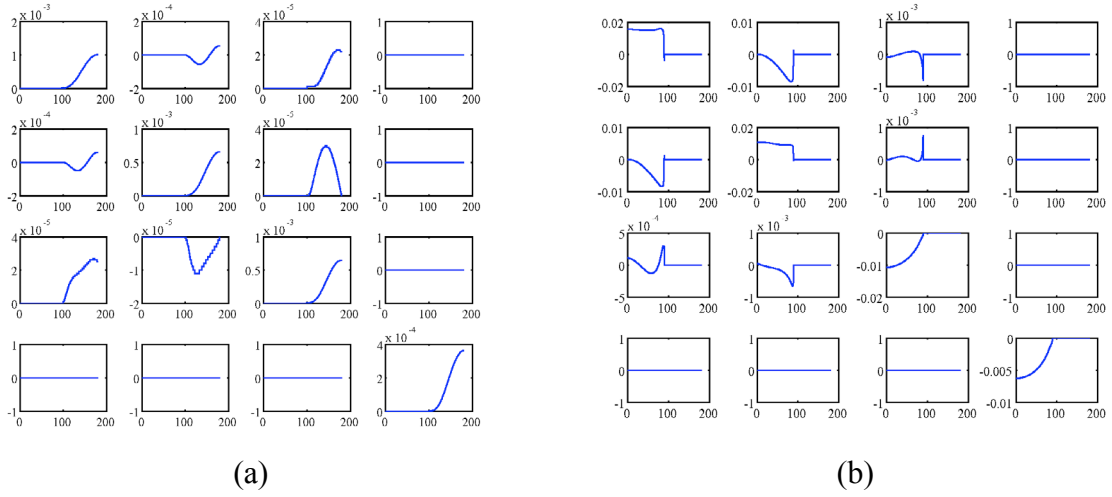


Fig. 14. Dependence of radiance on scattering angle at wavelength 587nm.
(a) $\tau = 0$, Sensor located at bottom of model. (b) $\tau = 5$, Sensor located at surface

In Fig. 5, we have shown the 16 elements of Mueller matrix for Raman scattering. Raman scattering has output from 565nm to 595nm. Here we only take the output of 587nm as an example. In the left figure, we place the sensor at the bottom of the seawater, and in the right figure, the sensor is at the top of the seawater. In our model, the total optical depth of seawater is 5. It is very clear that when the sensor is put at the top of the seawater, there is a significant scattering part, and when the sensor is located at the bottom of seawater, there is weak transmission only.

To show more information about the effect of optical depth on Raman scattering, we can take the P_{11} element as an example. Fig 6 shows the dependence of P_{11} on scattering angle at 6 different optical depths.

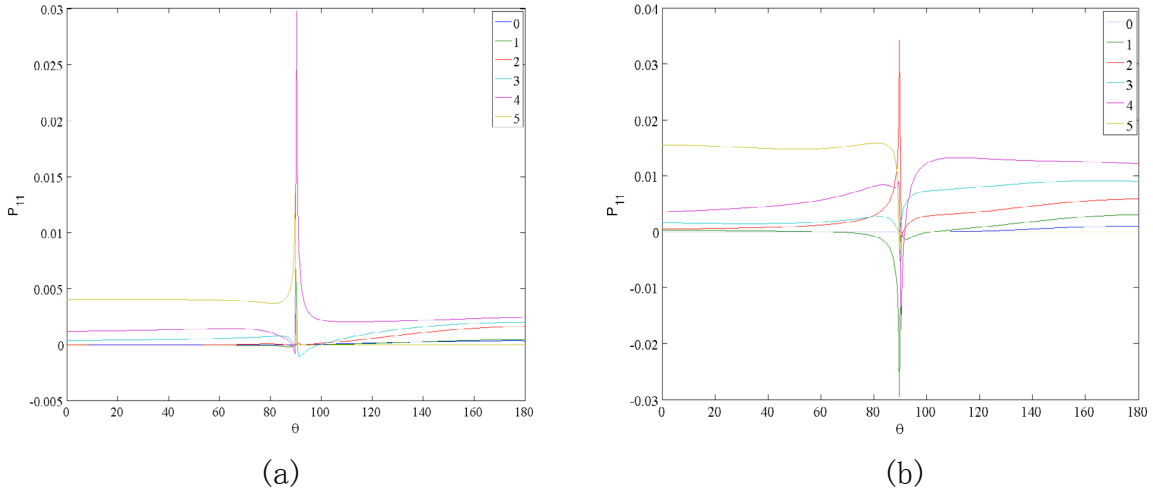


Fig. 6 Dependence of radiance on scattering angle at different optical depths.
(a) $\lambda = 575nm$ (b) $\lambda = 587nm$.

We can also show the dependence of radiance on both scattering angle and depth in a 3D figure, as shown in Fig. 7 a. We can see that, at around 90° , there are large statistical fluctuations; if we reduce the fluctuations by processing more histories, the relationship is clearer (Fig.7b).

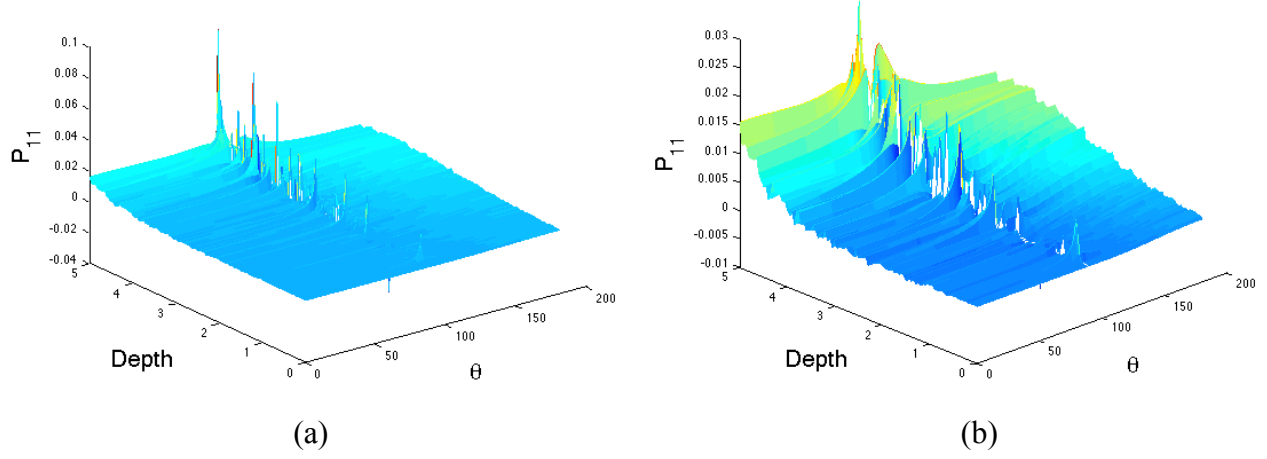


Fig. 7 Dependence of Radiance on both depth and scattering angle.

It is interesting to see that the transmission and scattering parts of the radiance have very different dependence on depth, as shown in Fig. 8. These can be explained by the fact that our light source is below air-sea surface, and the sensor will only record the scattered Raman light. As the first scattering is Raman scattering, when the sensor is closely located below the surface, there is certainly no scattered light but only incident light.

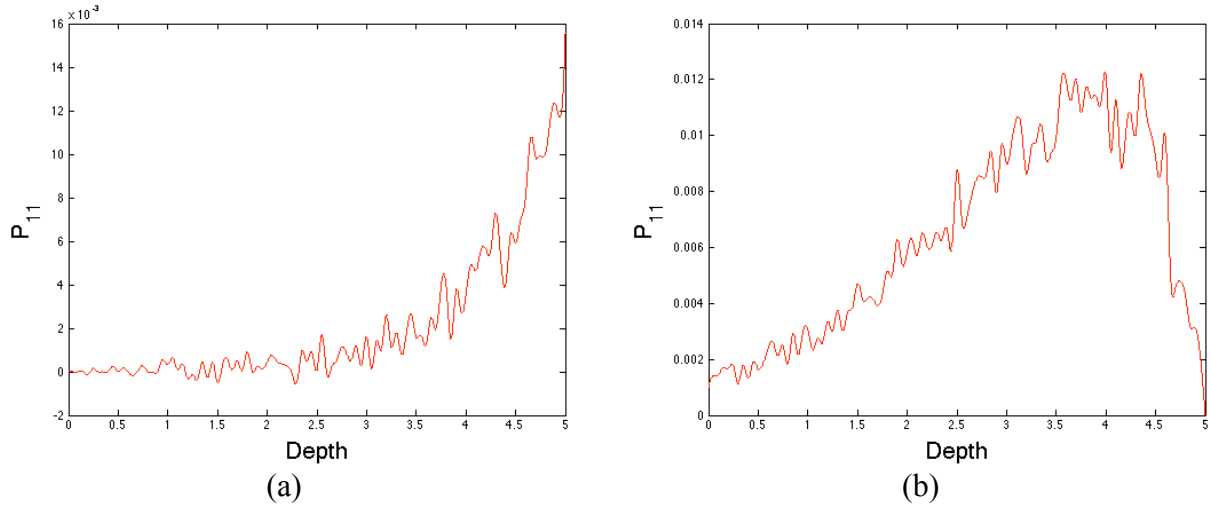


Fig. 8 Dependence of Scattering and Transmission part of radiance on depth
(a) P_{11} at 0° (scattering) (b) P_{11} at 180° (transmission)

The more interesting part is the change of Raman scattering distribution shape after multiple scattering. In our model, only the first scattering is Raman scattering. After that, each different wavelength output will go through Rayleigh scattering. It is known that different wavelengths have different absorption and scattering coefficients, which will result in the change of the band shape. As shown in Fig. 9, Raman scattering has a continuous band. We can only pick several scattered wavelengths to represent this shape. In our simulation, we take these wavelengths as $\lambda = 567, 571, 575, 579, 583, 587, 591, 595, 599$ nm. The new representative Raman scattering shapes are demonstrated in Fig. 9(a).

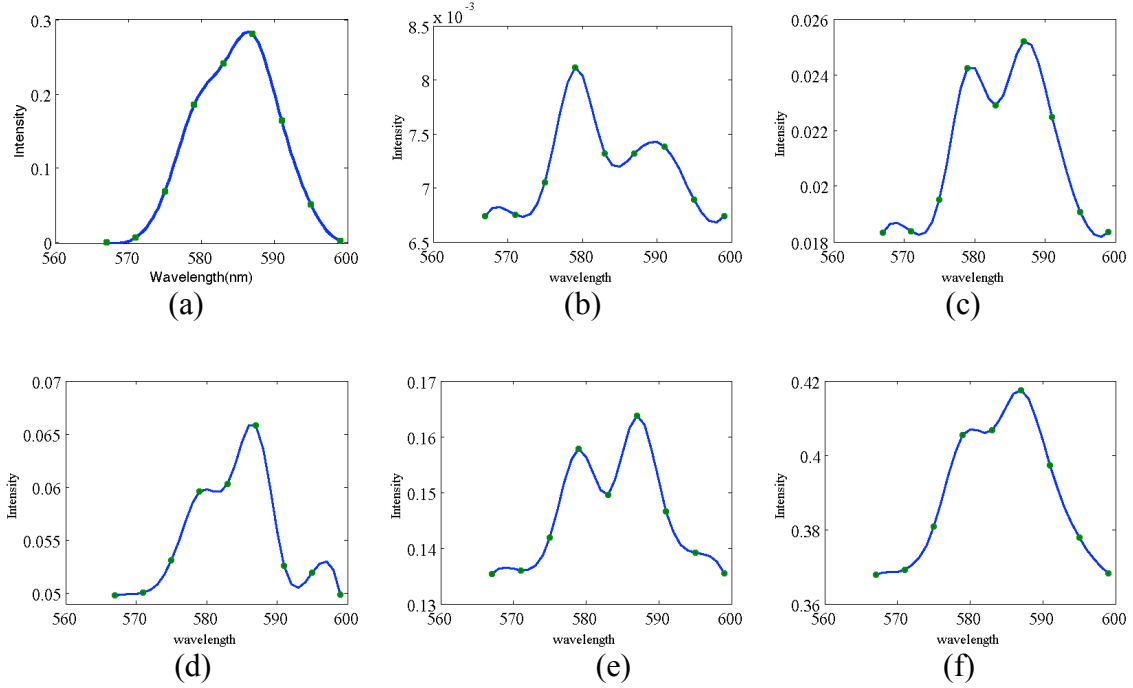


Fig. 9 (a) band shape of Single Raman scattering. (b)-(f) Raman band shape after multiple Rayleigh scattering. From (b)-(f), their optical depths are $\tau = 4, 3, 2, 1, 0$.

It is clear to see that with decreasing optical depth, the intensity increases correspondingly. One special phenomenon is that in Fig. 9(b), the shoulder shifts from the left side to the right side of the intensity peak. This definitely shows there are interesting things to further study.

IMPACT/APPLICATION

The HMOMC code and the fast irradiance code will become powerful tools to investigate the effects of a dynamic wave profile on the radiance field, especially on the polarization states and fast fluctuations of the light field. The fast irradiance code will also be helpful in understanding the fast-varying environment surrounding ocean organisms, which is part of an ONR funded MURI project on underwater camouflage.

TRANSITIONS

We will now add these new Raman scattering calculations to our underwater 3D code as part of our MURI project.

RELATED PROJECTS

We use the results from our other ONR Grant to use as input to our codes in our MURI study of cephalopods.

REFERENCES

1. G. W. Kattawar and G. N. Plass, "Asymptotic Radiance and Polarization in Optically Thick Media: Ocean and Clouds," *Appl. Opt.* 5, 3166-3178 (1976).
2. L. G. Stenholm, H. Störzer, and R. Wehrse, "An efficient method for the solution of 3-D Radiative Transfer Problems", *JQSRT.* 45. 47-56, (1991)
3. A. Sánchez, T.F. Smith, and W. F. Krajewski "A three-dimensional atmospheric radiative transfer model based on the discrete ordinates method", *Atmos. Res.* 33, 283-308, (1994),
4. J. L. Haferman, T. F. Smith, and W. F. Krajewski, "A Multi-dimensional Discrete Ordinates Method for Polarized Radiative Transfer, Part I: Validation for Randomly Oriented Axisymmetric Particles", *JQSRT*, 58379-398, (1997)
5. K.F. Evans, "The spherical Harmonics Discrete Ordinates Method for Three-Dimensional Atmospheric Radiative Transfer", *J. Atmos. Sci.*, 55, 429-446, (1998)
6. Q. Liu, C. Simmer, and E. Ruprecht, "Three-dimensional radiative transfer effects of clouds in the microwave spectral range", *J. Geophys. Res.* 101(D2), 4289-4298, (1996)
7. B. Mayer, "I3RC phase I results from the MYSTIC Monte Carlo model", Extended abstract for the I3RC workshop, Tucson Arizona, 1-6, November 17-19, (1999).
8. L. Roberti and C. Kummerow, "Monte Carlo calculations of polarized microwave radiation emerging from cloud structures", *J. Geophys. Res.* 104(D2), 2093-2104, (1999).
9. C. Davis, C. Emde, and R. Harwood, "A 3D Polarized Reversed Monte Carlo Radiative Transfer Model for mm and sub-mm Passive Remote Sensing in Cloudy Atmospheres", *Trans. Geophys. and Rem. Sens.*, Special MicroRad04 Issue, (2004).
10. G. N. Plass, G. W. Kattawar and F. E. Catchings, "Matrix Operator Theory of Radiative Transfer I. Rayleigh Scattering," *Appl. Opt.* 12, 314-329 (1973).
11. G. W. Kattawar, G. N. Plass and F. E. Catchings, "Matrix Operator Theory of Radiative Transfer. II. Scattering from Maritime Haze," *Appl. Opt.* 12, 1071-1084 (1973).
12. G. E. Walrafen, "Raman spectral studies of the effects of temperature on water structure," *The J. of Chem. Phys.* 47, 114 (1967).
13. X. Xu, "Significance of Raman Scattering in the ocean," dissertation (Texas A&M University 1994).

PUBLICATIONS

Kattawar, G.W. , “Genesis and Evolution of Polarization of Light in the Ocean”. Accepted for publication in Applied Optics [in press, refereed]

HONORS/AWARDS/PRIZES:

Recognized by Applied Optics as the 3rd most prolific author over the past 50 years